Formation of Grain Boundary α in β Ti Alloys: Its Role in Deformation and Fracture Behavior of These Alloys

JOHN W. FOLTZ, BRIAN WELK, PETER C. COLLINS, HAMISH L. FRASER, and JAMES C. WILLIAMS

Beta-Ti alloys contain sufficient concentrations of β stabilizing alloy additions to permit retention of the metastable β phase after cooling to room temperature. Decomposition of the metastable β phase results in the formation of several possible phases, at least two of which are metastable. Concurrently, equilibrium α phase often forms first by heterogeneous nucleation at the α grain boundaries with an accompanying precipitate free zone observed adjacent to the grain boundary α. The grain boundary regions are softer than the precipitation hardened matrix. As a consequence, fracture follows the prior β grain boundaries, especially in high-strength conditions. This fracture mode results in low tensile ductility and/or fracture toughness. This article will describe methods of minimizing or eliminating grain boundary α formation by using metastable transition precipitates to nucleate α more rapidly. The effects on fracture behavior also will be described.

DOI: 10.1007/s11661-010-0322-3

I. INTRODUCTION

BETA Ti alloys are commonly used in two microstructural conditions: fully lamellar and bimodal. In the bimodal condition, the material is hot worked in the $\alpha + \beta$ phase field to minimize grain boundary α (GBA) through recrystallization of both the α and β phases. The bimodal condition is used for applications that require higher strength. The combinations of strength and ductility that can be achieved in these alloys varies widely, which allows tailoring of properties for specific applications. In the fully lamellar conditions, it is well known that continuous layers of α phase at prior beta grain boundaries can be deleterious to mechanical properties in both $\alpha + \beta$ and β classes of titanium alloys.[1–4]

Nucleation of the α phase in the fully lamellar microstructure typically begins at the prior β grain boundaries.[5] Sympathetic nucleation and growth of Widmanstätten α from the grain boundary then populates the interior of the grain with this phase. However, population of the β grain interiors with α phase precipitates can occur by other mechanisms, as others have discussed.[6–9] For example, in many binary titanium alloys, the α phase can nucleate and grow from metastable β phase decomposition products, either ω or β' phases.[6] The operative mechanism strongly depends on the parent β-phase composition. In this case, the number of α–phase nucleation sites can substantially increase, resulting in a general refinement of the microstructural scale, including α lath size.

The creation of alternative nucleation sites through thermal treatments can refine lath size, as well as potentially decrease the thickness and continuity of the typically continuous GBA layers. This article explores a way in which GBA can be reduced or eliminated through controlled use of metastable phases in a particular β-titanium alloy: Ti-5Al-5Mo-5V-3Cr-0.5Fe (Ti-5553). Fractographic observations and mechanical properties of a thermal treatment containing a small amount of GBA also will be discussed.

II. EXPERIMENTAL PROCEDURE

Two bars of Ti-5553 were solutionized at 50 K above the α/β transus, 1183 K (910 °C), step cooled to 813 K (540 °C) and aged for 2 hours, upquenched to 923 K (650 °C) and aged for 2 hours, and finally cooled to room temperature. The thermal treatment was conducted in a Gleeble 1500 thermo-mechanical simulator (Gleeble, Dynamic Systems, Poestenkill, NY) with a vacuum of $<10^{-3}$ Pa. The thermal history of the 89 mm × 9 mm × 9 mm bars is shown in Figure 1. The heat-treated bars were cut using wire electrodischarge machining (EDM) and subjected to two series of mechanical tests.

In the first series of tests, the flat dog-bone-shaped samples were cut and polished to a finish of 800 grit with silicon carbide papers, then enamel painted with a speckle pattern of black dots on a white background. The 40-mm long samples measured approximately 2 mm × 1 mm within the gauge section, and 3 mm × 1 mm in the grips. Tensile tests were performed on an Instron ETMT (ETMT; Instron, Norwood, MA)

JOHN W. FOLTZ, Graduate Research Associate, BRIAN WELK, Research Scientist, HAMISH L. FRASER, Ohio Regents Eminent Scholar, and JAMES C. WILLIAMS, Professor, are with The Ohio State University, Columbus, OH 43210. Contact e-mail: foltz@matsceng.ohio-state.edu PETER C. COLLINS, Director of Technology, is with Quad Cities Manufacturing Laboratory, Arsenal Rock Island, Moline, IL 61201.

Manuscript submitted January 8, 2010.
Article published online June 5, 2010

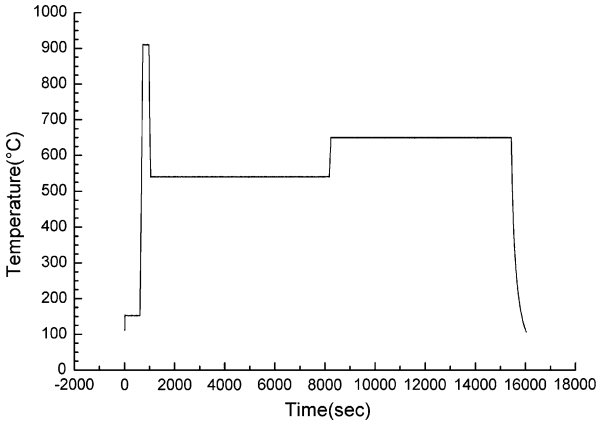

Fig. 1—Ti-5553 solution heat treated at 1183 K (910 °C) for 5 minutes, step cooled to 813 K (540 °C) and aged for 2 hours, then upquenched to 923 K (650 °C) and aged for 2 hours.

mechanical tester in a similar fashion to the work of Peterson *et al.*,[10] at a displacement rate of 1.17 μm/s in the gauge section, with a rate jump after 240 seconds to 11.67 μm/s (approximately 8×10^{-5} s^{-1} and 8×10^{-4} s^{-1}, respectively). Strain was measured using digital image correlation with the painted speckle pattern within the gauge length.

The second series of tests conducted were four-point bend fatigue tests, similar to those described by Pilchak *et al.*[4] Following the works of both Pilchak *et al.*[11] and Zhai *et al.*,[12] the inner and outer pin spacings were matched to the sample thickness such that a uniform tensile stress was predicted between the inner pins on the tensile face. The fixture includes a spherical bearing to prevent off-axis loading. The top surfaces of the samples were polished to 0.05 μm colloidal silica, whereas the sides and corners of the samples were grit blasted to prevent corner crack initiation. The tests were conducted at 60 Hz at an R value of 0.1, with a maximum tensile stress at the surface equal to 1092 MPa.

The microstructures of the various samples were characterized by conducting stereological measurements on polished samples made from untested material. Ten images similar to Figure 2 were acquired to quantify the microstructure using a scanning electron microscopy (SEM) equipped with a field emission electron gun operating at an accelerating voltage of 10 keV, using a backscattered electron detector. Grain size was determined using ASTM Specification E112-96, and other features were quantified using the method described in Reference 13. The measured average value of grain size, mean intercept length, was 76 microns (ASTM grain size 4). The calculated α phase fraction was 40.1 pct, the average α lath thickness was 0.06 microns, and the mean distance between laths was 0.07 microns.

Post fracture analysis was conducted using a suite of electron microscopes. Electron backscattered diffraction (EBSD) scans and fractographic analysis were performed using an SEM operating at 25 keV. Transmission electron foils were excised from bulk samples using a FEI Helios 600 dual beam SEM/FIB (Helios; FEI Company, Hillsboro, OR) operating with an ion

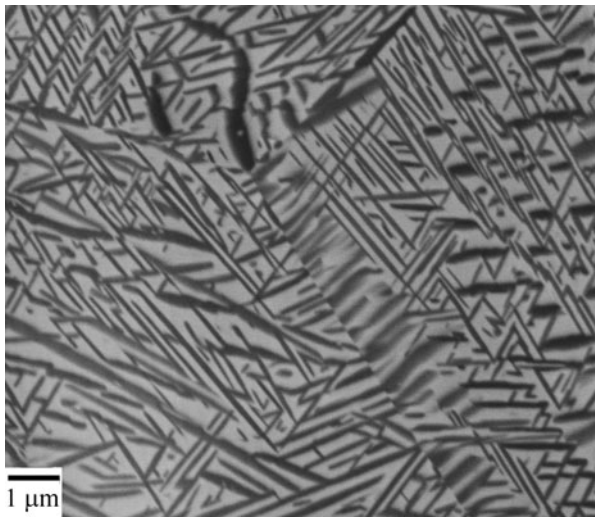

Fig. 2—Backscattered electron image of microstructure. A triple point is shown in the upper left of the image, and no GBA is visible at the SEM resolution.

Table I. Mechanical Properties of Heat-Treated Ti-5553

Sample Number	0.2 pct Offset Yield Strength (MPa)	Ultimate Tensile Strength (MPa)	Strain to Fail (pct)
1	1217	1311	7.8
2	1191	1268	5.41
3	1253	1327	4.44
4	1176	1278	7.32
5	1246	1329	5.66
6	1199	1299	8.8
Average/standard deviation	1214/31	1302/25	6.6/1.7

potential of 30 keV, to investigate the nature and presence of GBA. Scanning transmission electron microscopy (STEM) analysis was completed using a FEI Tecnai F20 (Tecnai; FEI Company). Images were collected using the high-angle annular dark field detector (HAADF) at a camera length of 54 mm to observe the morphology and presence of α and β phases using atomic number contrast by elemental partitioning.[14]

III. RESULTS AND DISCUSSION

The results of six tensile tests are shown in Table I. Average yield strength of 1214 MPa was measured, along with an average ultimate tensile strength of 1302 MPa. The average lifetime of the four fatigue tests conducted at a maximum stress equal to 1092 MPa, or approximately 90 pct of the yield strength, was 22,807 cycles.

Figure 3 shows a grain boundary region as observed in STEM HAADF. Here, it is clear that the presence of GBA is limited and, where present, it is discontinuous. Despite this, some α lamellae seem to have grown from the grain boundary regions toward the grain interiors.

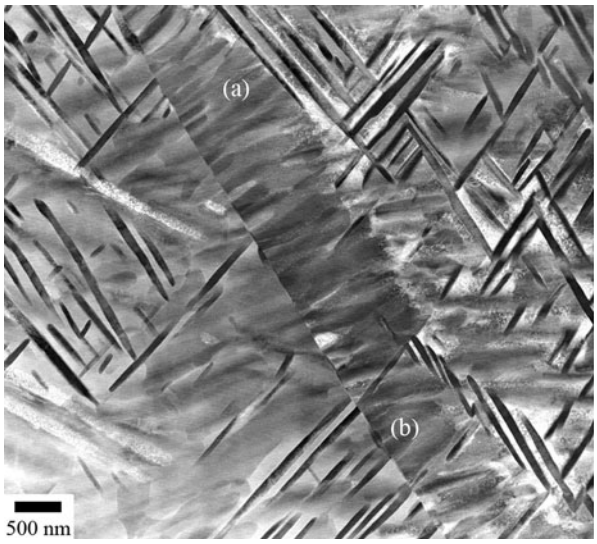

Fig. 3—HAADF STEM image of as-heat treated condition of Ti-5553. (*a*) Widmanstätten α is visible to the right of the grain boundary, despite no continuous layer of GBA. (*b*) The GBA present is in the form of discrete precipitates.

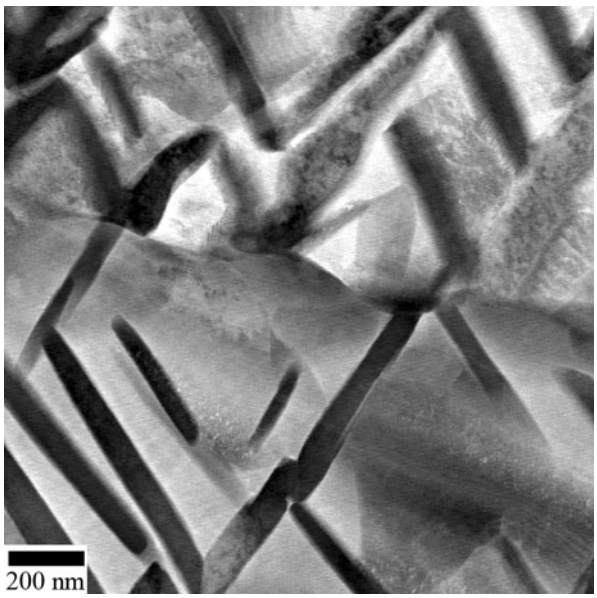

Fig. 4—High-magnification STEM image taken across a grain boundary with a HAADF detector. Although lamellae seem to intersect the grain boundary, no continuous layer of GBA is present.

The presence of classic grain boundary α films seems to be limited even when imaged at higher magnification, as shown in Figure 4. Although the α lamellae do intersect the boundary, there is little GBA formation.

Fractographic examination showed a mixed mode of intergranular and transgranular fracture in both failed tensile specimens (Figure 5) and in failed fatigue specimens (Figure 6). Surface crack initiation was observed in all fatigue tests, which corresponds to the region of highest maximum bending stress. In regions of intergranular fracture within the tensile samples, it should be noted that failure occurred by microvoid nucleation and

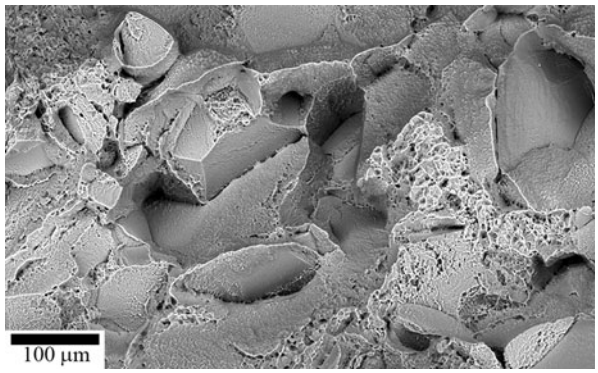

Fig. 5—Fracture surface from one tensile test. Significant amounts of intergranular fracture occurred.

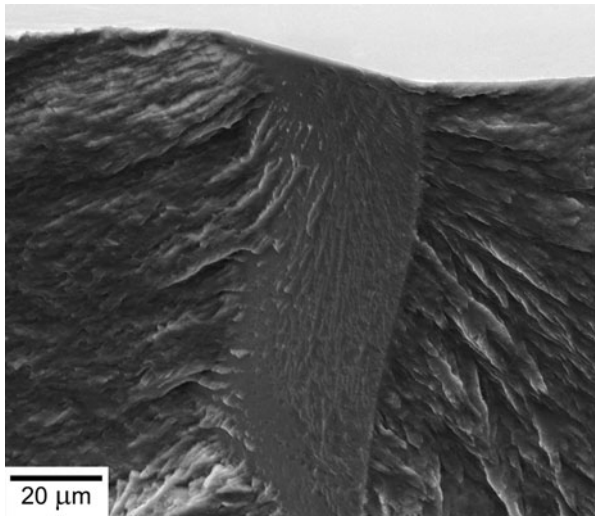

Fig. 6—Fracture surface of the crack initiation site in a four-point bending fatigue test. Image was collected with a 70-deg tilt in the vertical direction with respect to the normal of the polished face shown in the upper portion of the image.

coalescence along the grain boundaries. The small size of these microvoids suggests that the plastic zone was constrained geometrically to near the grain boundary region.

Fatigue crack initiation in α + β and metastable β Ti alloys has been linked with GBA by others.[2,4,15,16] For this reason, it is important to understand how to control the amount of GBA. Figure 3 shows how Widmanstätten α phase can grow with similar growth directions from a β grain boundary that lacks a significant amount of GBA. In fact, GBA was found in relatively few locations while inspecting the grain boundaries at high magnification; one such area is highlighted Figure 3(b). As shown, this GBA appears as discrete discontinuous precipitates located within the grain boundary, but these are unlike either the lenticular α precipitates that appear to be perpendicular to the grain boundary or the continuous GBA found in other titanium microstructures. The reasons for these differences are the subject of ongoing study.

The crack initiation was easily identifiable by the smooth nature of the facet and the chevron markings

indicating the direction of crack growth. After SEM inspection of the polished face adjacent to the crack initiation site (Figures 7 and 8), it seems that while continuous GBA is minimized, it is not eliminated completely. Grain boundary crack initiation sites have been reported commonly in the literature and are theorized to be caused by differences in the elastic-plastic response between grains.[17–19] These differences, along with the stress distributions near the grain boundary versus the grain interior, can cause the plastic zone to be constrained mechanically to near the grain interface.

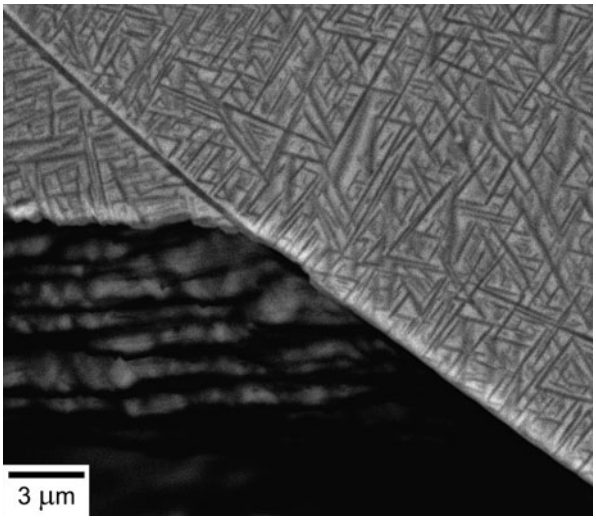

Fig. 7—Secondary electron image of the polished surface adjacent to fatigue crack initiation.

Quantitative tilt fractography was used to calculate the angular deviation between the loading direction and the initiation facet normal, in a similar fashion to other authors.[18,20,21] The measured angle of the facet was 39.97 deg with respect to the loading axis, which is in the range of angles observed in many fatigue failures.[4] As discussed by Pilchak *et al.*,[4] facets that deviate up to 15 deg from the maximum shear direction of 45 deg contain both large normal and shear forces. Based on theories proposed by others, both of these force components are necessary to initiate cracks in titanium alloys.[19,22]

Because of the size of the alpha precipitates, no crystallographic information could be detected using EBSD from the GBA. Instead, the β-phase orientation information was used to investigate the crystallographic nature of the initiation facet (Figure 8). Using EBSD data and the facet normal, it was calculated that the facet is within the experimental error from a {110} plane on the right grain (Figure 9).[23] The orientation of the left grain seems to be far from any slip planes, unlike the right grain. If the observed GBA on the facet shared a Burgers orientation relationship with the right grain, this could suggest that its basal plane was aligned with the initiation facet. Other researchers have shown that GBA can initiate cracks along the basal plane.[4,22,24]

There are two important implications of the grain boundary crack initiation: β-grain boundaries are the

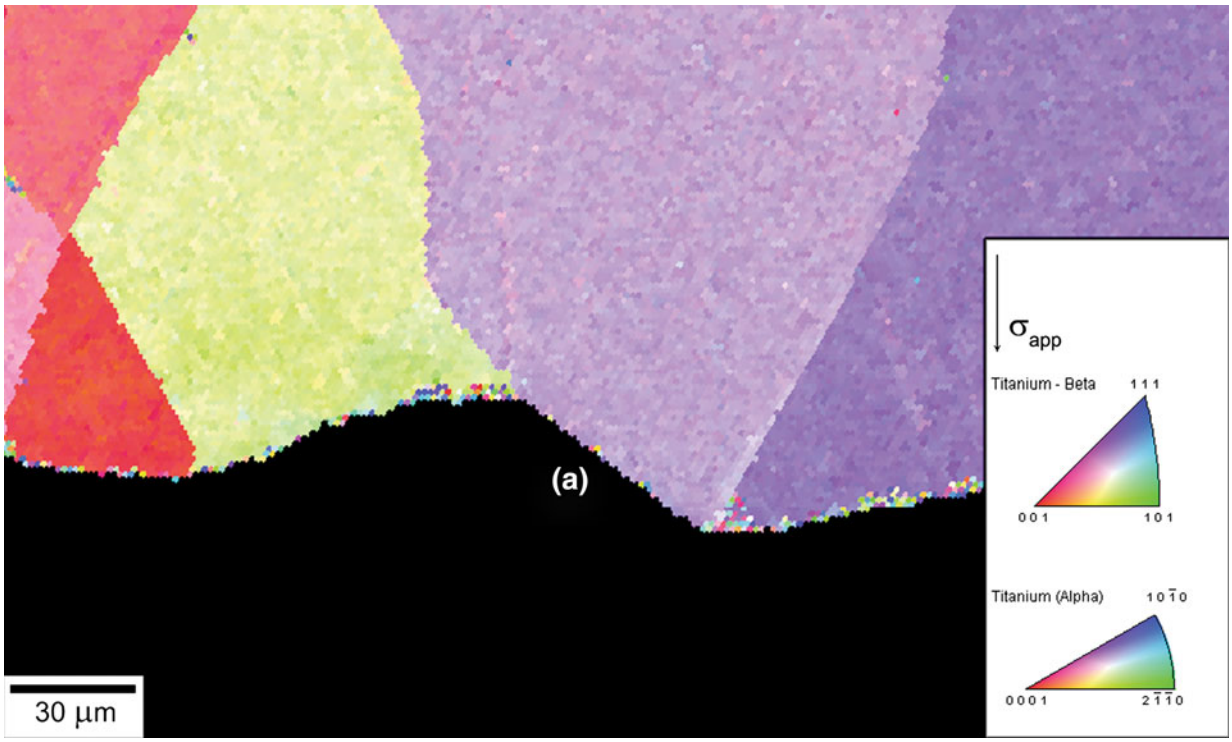

Fig. 8—EBSD map showing one half of the crack initiation site, located at (*a*). The initiation site occurred at the surface of the sample, along a grain boundary. A combination of transgranular and intergranular fracture is observed in the image.

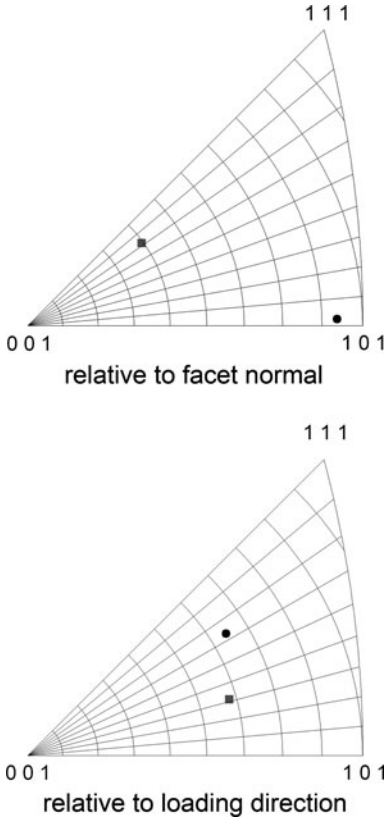

Fig. 9—Equal-angle inverse pole figures showing orientation of the β phase relative to (top) the facet normal and (bottom) loading direction (001). The left grain in Fig. 8(a) is shown by the gray square, and the right grain is shown with the black circle.

weakest microstructural feature in this microstructural condition, and GBA can be minimized but is unlikely to be altogether eliminated with aging treatments similar to this study. This observation becomes especially important in understanding the low ductility values typically obtained in high-strength β alloys in the fully lamellar condition.

Tensile ductility remains low in the tested condition despite reduction in GBA. Conventional wisdom is that continuous layers of GBA allow cracks to move through the grain boundary regions with little resistance. However, another underlying mechanism, such as oxygen enrichment at grain boundaries, could also explain this behavior when GBA is reduced or eliminated.

Work by Wu *et al.*[25] has also shown that GBA can be reduced through small alloying additions of carbon. They observed via WDS that in alloys without carbon, higher amounts of oxygen are detectable at the grain boundary than within the grain interiors. In contrast, the oxygen content remains uniform throughout grain interiors and boundaries when carbon is added to the alloy. These carbon-containing alloys maintain ductility, even in high strength conditions, which they believe is related to oxygen content at the grain boundary.[26] This opens carbon additions as an attractive avenue to minimize GBA while improving ductility in deep hardened conditions for β titanium alloys.

It seems that metastable phases can aid nucleation of α phase in heavily stabilized β titanium alloys.[9,27,28] Thermal treatments that take advantage of uniform, intragranular nucleation sites can create a fine dispersion of lamellae within the prior beta grain. In principle, the α phase could then be aged at a higher temperature to coarsen the lamellae while minimizing any formation of GBA. The coarsening rates could be reduced, however, by the large solute diffusion lengths necessary.

IV. CONCLUSIONS

1. Grain boundary α can be deleterious to mechanical properties in β alloys.
2. Crack initiation occurred along a grain boundary, and was aligned near a {110} of one grain.
3. The facet was aligned for a combination of high shear with normal forces, suggesting that both shear and normal force components are necessary to initiate a crack. This finding is consistent with the observations of other authors.
4. From fractographic examination, the plastic zone near the initiation site is constrained mechanically to the region encompassing the GBA, possibly because of differences in elastic-plastic response.
5. Low ductility is observed still in high-strength conditions that lack significant amounts of grain boundary α.

ACKNOWLEDGMENTS

Support for this work is gratefully acknowledged from the U.S. Office of Naval Research D3-D program, Grant. N00014-05-1-0504. The authors would like to thank Adam Pilchak for his valuable discussions.

REFERENCES

1. U. Krupp, W. Floer, J.F. Lei, Y.M. Hu, H.J. Christ, A. Schick, and C.P. Fritzen: *Philos. Mag.*, 2002, vol. 82 (17/18), pp. 3321–32.
2. G. Lütjering, J. Albrecht, C. Sauer, and T. Krull: *Mater. Sci. Eng., A.*, 2007, vols. 468–470 (Special Issue SI), pp. 201–09.
3. J.O. Peters and G. Lütjering: *Metall. Mater. Trans. A.*, 2001, vol. 32A, pp. 2805–18.
4. A.L. Pilchak, R.E.A. Williams, and J.C. Williams: *Metall. Mater. Trans. A.*, 2010, vol. 41A, pp. 106–24.
5. J.C. Williams and G. Lütjering: *Titanium*, 2nd ed., Springer, Berlin, Germany, 2007, p. 32.
6. S. Nag, R. Banerjee, R. Srinivasan, J.Y. Hwang, M. Harper, and H.L. Fraser: *Acta Mater.*, 2009, vol. 57 (7), pp. 2136–47.
7. F. Prima, P. Vermaut, G. Texier, D. Ansel, and T. Gloriant: *Scripta Mater.*, 2006, vol. 54 (4), pp. 645–48.
8. J.C. Williams: *The Science Technology and Applications of Titanium*, Plenum Press, New York, NY, 1973, pp. 1433–94.
9. S.Z. Zhang, Z.Q. Liu, G.D. Wang, L.Q. Chen, X.H. Liu, and R. Yang: *J. Cent. South Univ. Technol.*, 2009, vol. 16 (3), pp. 354–59.
10. B. Peterson, P.C. Collins, and H.L. Fraser: *Mater. Sci. Eng. A*, 2009, vols. 513–514, pp. 357–65.
11. A.L. Pilchak, D.M. Norfleet, M.C. Juhas, and J.C. Williams: *Metall. Mater. Trans.*, 2008, vol. 39A, pp. 1519–24.
12. T. Zhai, Y.G. Xu, J.W. Martin, A.J. Wilkinson, and G.A.D. Briggs: *Int. J. Fatig.*, 1999, vol. 21 (9), pp. 889–94.
13. P.C. Collins, B. Welk, T. Searles, J. Tiley, J.C. Russ, and H.L. Fraser: *Mater. Sci. Eng. A.*, 2009, vol. 508 (1–2), pp. 174–82.

14. L. Kovarik, S.A. Court, H.L. Fraser, and M.J. Mills: *Acta Mater.*, 2008, vol. 56 (17), pp. 4804–15.
15. C. Sauer and G. Lütjering: *Mater. Sci. Eng. A.*, 2001, vol. 319 (Special Issue SI), pp. 393–97.
16. K. Tokaji, K. Ohya, and H. Kariya: *Fatigue Frac. Eng. Mater. Struct.*, 2000, vol. 23 (9), pp. 759–66.
17. Y.M. Hu, W. Floer, U. Krupp, and H.J. Christ: *Mater. Sci. Eng. A.*, 2000, vol. 278 (1–2), pp. 170–80.
18. V. Sinha, M.J. Mills, and J.C. Williams: *J. Mater. Sci.*, 2007, vol. 42 (19), pp. 8334–41.
19. A.P. Woodfield, M.D. Gorman, J.A. Sutliff, and R.R. Corderman: in *Fatigue Behavior of Titanium Alloys*, R.R. Boyer, D. Eylon, and G. Lütjering, eds., TMS, Warrendale, PA, 1999, pp. 111–18.
20. A.L Pilchak and J.C. Williams: *Metall. Mater. Trans. A.*, 2010, vol. 41A, pp. 22–25.
21. D.C. Slavik, J.A. Wert, and R.P. Gangloff: *J. Mater. Res.*, 1993, vol. 8 (10), pp. 2482–91.
22. V. Sinha, M.J. Mills, and J.C. Williams: *Metall. Mater. Trans. A.*, 2006, vol. 37A, pp. 2015–26.
23. Y.J. Ro, S.R. Agnew, and R.P. Gangloff: *Scripta Mater.*, 2005, vol. 52 (6), pp. 531–36.
24. C.C. Wojcik, K.S. Chan, and D.A. Koss: *Acta Metall.*, 1988, vol. 36 (5), pp. 1261–70.
25. X.H. Wu, J. del Prado, Q. Li, A. Huang, D. Hu, and M.H. Loretto: *Acta Mater.*, 2006, vol. 54 (20), pp. 5233–48.
26. M. Chu, X. Wu, I.P. Jones, and M.H. Loretto: *Mater. Sci. Technol.*, 2006, vol. 22 (6), pp. 661–66.
27. J.C. Williams and M.J. Blackburn: *Trans. Metall. Soc. AIME*, 1969, vol. 245 (10), pp. 2352–55.
28. J.C. Williams, B.S. Hickman, and H.L. Marcus: *Metall. Trans.*, 1971, vol. 2, p. 1913.